19

Silicon Carbide Filled Polymer Composite for Erosive Environment Application: A Comparative Analysis of Experimental and FE Simulation Results

Sandhyarani Biswas[1], Amar Patnaik[2] and Pradeep Kumar[2]
[1]*Department of Mechanical Engineering, National Institute of Technology, Rourkela,*
[2]*Department of Mechanical Engineering, National Institute of Technology, Hamirpur,*
India

1. Introduction

Polymer composites form important class of engineering materials and are commonly used in mechanical components. Because of their high strength-to-weight and stiffness-to-weight ratios, they are extensively used for a wide variety of structural applications as in aerospace, automotive, gear pumps handling industrial fluids, cams, power plants, bushes, bearing cages and chemical industries. Whereas, wear performance in nonlubricated condition is a key factor for the material selection and fabrication procedure (Hutchings, 1992). Glass fiber reinforced polymer composites traditionally show poor wear resistance due to the brittle nature of the fibers. Many researchers have been reported on the effect of fiber, filler and matrix materials so far in the literature regarding economical and functional benefits to both consumers and industrial manufacturers (Budinski, 1997; Chand et al., 2000; Tripathy and Furey, 1993). The addition of hard particulate ceramic fillers not only improves the wear performance of the particulate filled polymer composites but also reduce the cost of the composites. In order to obtain improve wear performances many researchers modified polymers using different fillers (Briscoe et al. 1974; Tanaka 1986; Bahadur et al, 1994; Bahadur and Tabor,1985; Kishore et al. 2000; Wang et al. 2003).

Silicon carbide (SiC) is one such ceramic material that has great potential for overcoming the current inadequacies of abrasive products due to its inherent characteristic of being chemically inert and consequently resistant to improve mechanical and wear resistance material. It has an excellent abrasive nature and has been produced for grinding wheels and other for more than hundred years. Now-a-days the material has been developed into a high quality technical grade ceramic with very good mechanical properties. It is used in abrasives, ceramics, refractories, and other high-performance applications. Silicon carbide is composed of tetrahedra of carbon and silicon atoms with strong bonds in the crystal lattice. This produces a very strong material and not attacked by any acids or alkalis or molten salts up to 800°C (Nordsletten et al. 1996).

To this end, the present research work is undertaken to develop a new class of glass fiber based polymer composite filled with SiC particulate and study the effect of various operational variables, material parameters and their interactive influences on erosive wear behavior of these composites. A finite element (FE) model (AUTO-DYN) of erosive wear is established for damage assessment and validated by a well designed set of experiments. The eroded surfaces of these composites are analyzed with scanning electron microscopy (SEM), and the erosion wear mechanisms of the composites are investigated.

2. Experimental

2.1 Preparation of composites

In this study, short E-glass fiber with 6mm length (Elastic modulus of 72.5 GPa and density of 2.59 gm/cc) is taken to prepare all the particulate filled (SiC) glass fiber reinforced polyester composites. The unsaturated isophthalic polyester resin (Elastic modulus 3.25GPa and density 1.35gm/cc) is manufactured by Ciba Geigy and locally supplied by Northern Polymers Ltd. New Delhi, India. The composite fabricated in two different parts. One part having different fiber loading with varying the fiber weight fraction from 10wt% to 50wt% at an increment of 10wt% and the second part, SiC filled short glass fiber reinforced polyester resin with three different percentages (0wt%, 10wt% and 20wt% of SiC). The mixture is poured into various moulds conforming to the requirements of various testing conditions and characterization standards. The entrapped air bubbles (if any) are removed carefully with a sliding roller and the mould is closed for curing at a temperature of 30°C for 24 h at a constant pressure of 10 kg/cm^2.

2.2 Air-jet erosion tester

The solid particle erosion test rig as per ASTM G76 used in the present study consists of an air compressor, a particle feeder, an air particle mixing chamber and accelerating chamber. The equipment was designed to feed erodent particles into a high velocity air stream, which propelled the particles against the specimen surface (Strzepa et al., 1993; Routbort et al., 1981). The erodent particles entrained in a stream of compressed air and accelerated down to a 65mm long brass nozzle with 3mm inside diameter to impact on a specimen mounted on an angle fixture. The velocity of the eroding particles is determined using rotating disc method (Ruff and Ives, 1975). The steady state erosion rate was determined by weighing the sample before and after the end of each test. While the impingement angles ranges from 30° to 90° and the test duration was 20min for each run. The erodent used for this test was river silica sand particle of three different sizes, i.e. 250, 350 and 450μm. The sample was cleaned with a blast of compressed air before each weighing to remove all loosely adhering debris. The mass loss from the target was measured with an analytical balance of ±0.01mg accuracy. The process is repeated every 10 minutes till the erosion rate attains a constant value called steady-state-erosion-rate. Finally, the worn surfaces of some selected samples are examined by scanning electron microscope JEOL JSM-6480LV.

2.3 Finite element model

In the present work, the erosive wear processes are modeled using an explicit dynamic code ANSYS/AUTO-DYN. The eight-node brick hexahedral elements with one integration point are used in the 3D simulation. The mesh is refined to a standard cubic element in order to calculate the erosion rate at the targeted area on the composites. It has been studied in literature that simulating a single particle was not sufficient to get valid results therefore subsequently considered three or more particles were needed to simulate the erosion process instead of single particle (ElTobgy et al., 2005). In this study, 125 spherical shaped particles were used to ensure the accuracy of the proposed model. All the particles are striking the target area at random locations. There are 10 groups which contain 125 particles aggregately in the proposed model.

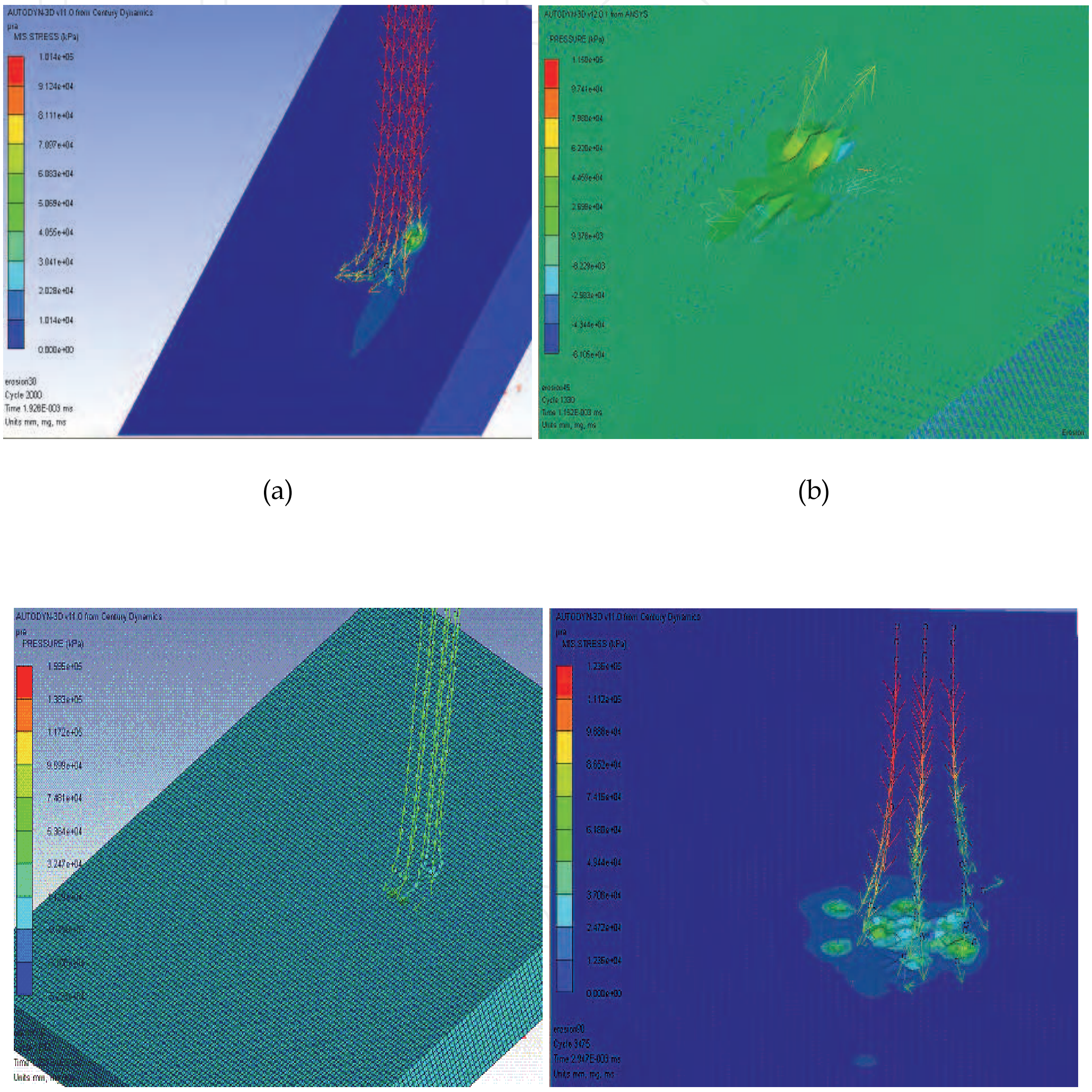

(a) (b)

(c) (d)

Fig. 1. Schematic diagram of target composite material and nozzle (a: 30° impingement angle, b: 45° impingement angle, c: 60° impingement angle and d: 90° impingement angle)

Each group has 12 particles which would impact the surface simultaneously and followed by another simultaneous particles group, and so on. According to the researchers, the distance between any two particles' centers in the same group is no less than 0.6r (r is the radius of the particles) to avoid the damage interaction (Woytowitz and Richman, 1999). The finite element model of the target material and simulated nozzle is shown in Figure 1. For the particles, the rotation degrees of freedom are constrained. Generally, the erosion rate (g/g) was used to characterize the erosion performance of the target materials.

2.4 Taguchi experimental design

Taguchi method is a statistical tool for the purpose of designing experimental procedure and mainly improving product quality. It uses the orthogonal array to set up the experiment for the advantages of less number and optimizes the process parameters by the analysis of signal-to-noise (SN) ratio. Taguchi method has become a powerful analysis tool for improving the experimental results to get high quality at low cost (Peace, 1993; Phadke, 1989). Therefore, a large number of factors are included so that non-significant variables can be identified at earliest opportunity. The impact of five such parameters are studied using L_{27} (3^{13}) orthogonal design. The operating conditions under which wear tests are carried out are given in Table 1. In conventional full factorial experiment design, it would require 3^5 = 273 runs to study five parameters each at three levels whereas, Taguchi's factorial experiment approach reduces it to only 27 runs offering a great advantage in terms of experimental time and cost. The experimental observations are further transformed into signal-to-noise (S/N) ratio. There are several S/N ratios available depending on the type of performance characteristics. The S/N ratio for minimum wear rate can be expressed as "lower is better" characteristic, which is calculated as logarithmic transformation of loss function as shown below (Peace, 1993).

Smaller is the better characteristic:

$$\frac{S}{N} = -10\log\frac{1}{n}\sum Y^2 \tag{1}$$

where, n the number of observations and y the observed experimental data.

The plan of the experiments is as follows: the first column is assigned to impact velocity (A), the second column to SiC content (B), the fifth column to impingement angle (C), the ninth column to stand-off distance (D) and the tenth column to erodent size (E), the third and fourth column are assigned to $(A\times B)_1$ and $(A\times B)_2$ respectively to estimate interaction between impact velocity (A) and SiC content (B), the sixth and seventh column are assigned to $(B\times C)_1$ and $(B\times C)_2$ respectively to estimate interaction between the SiC content (B) and impingement angle (C), the eight and eleventh column are assigned to $(A\times C)_1$ and $(A\times C)_2$ respectively to estimate interaction between the impact velocity (A) and impingement angle (C) and the remaining columns are used to estimate experimental errors. The output to be studied is erosion rate (E_r) and the tests are repeated twice corresponding to 54 tests. Furthermore, a statistical analysis of variance (ANOVA) is performed to identify the process parameters that are statistically significant. With the S/N and ANOVA analyses, the optimal combination of the process parameters can be predicted to a useful level of accuracy. Finally, a confirmation experiment is conducted to verify the optimal process parameters obtained from the parameter design.

Control factor	Level I	II	III	Units
A:Impact velocity	43	54	65	m/sec
B: SiC content	0	10	20	%
C:Impingement angle	30	60	90	Degree
D:Stand-off distance	65	75	85	mm
E:Erodent size	250	350	450	μm

Table 1. Levels for various control factors

3. Results and discussion

3.1 Erosive wear of the composites

The results have been organized and discussed in two sections. Firstly, the steady state erosion characteristics of the composites are determined for selected level of optimally controlled operating variables and compared the steady state results with the simple finite element simulation results to observe the variations in erosion rate with respective to impingement angle and the next, simulations results have been analyzed under Taguchi's experimental technique.

3.2 Steady state erosion rate

3.2.1 Influence of impingement angle

Solid-particle erosion is a complex wear phenomena influenced by a number of control factors such as impact velocity, angle of impingement, erodent particle size, stand-off-distance, materials properties, erodent particles geometry and environment temperature etc. Among these, impingement angle is the one of the most important parameter and widely studied parameter in the erosion study of materials (Hutchings, 1992; Tsuda et al., 2006). The erosion rate is measured of function of impingement angle, two types of material behavior generally observed in the target material i.e. ductile and brittle nature. The ductile nature of materials is characterized by maximum erosion rate at acute angle (15-30°) and for brittle behavior of materials, the maximum erosion rate is observed at normal impingement angle (90°). But as far as polymer matrix composites are concerned the composite materials show versatile in nature depending upon the fabrication procedure and type of reinforcing material. The reinforced composites show a semi-ductile behavior having the maximum erosion rate in the range of 45-60° (Hutchings, 1992), unlike the above two categories. This classification, however, is not absolute as the erosion of material has a strong dependence on erosion conditions such as the properties of target material.

In the present study of SiC filled glass fiber-polyester composites, the erosion rate increases monotonically with the increase in impingement angle and reaches maximum at 45° impingement angle for particulate filled composites. However, for unfilled composite the maximum erosion rate is found to be at 60° impingement angle. This indicated that all the particulate filled and unfilled composites show semi-ductile erosion behaviour irrespective of filler content. Similarly, the finite element analysis simulated results are in good agreement with the experimental results as observed in Figure 2. As far as erosion resistance is concerned 20wt% SiC filled composites show better erosion resistance among other particulate filled and unfilled composites. Whereas, unfilled composites shows maximum erosion rate as compared with 10wt% and 20wt% SiC filled glass fiber reinforced polyester composites both in experimental and finite element analysis simulated results as shown in Figure 2.

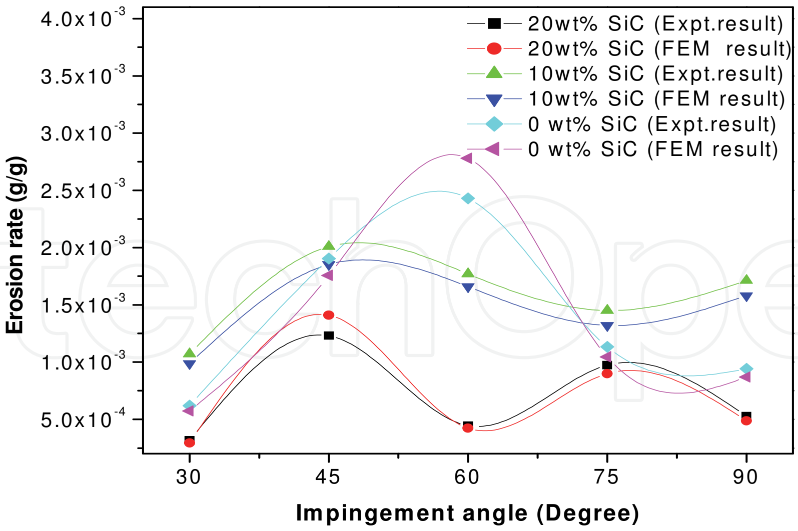

(Impact velocity: 43 m/sec, stand-off distance: 75mm and erodent size: 450μm)

Fig. 2. Influence of impingement angle on erosion rates of composites

3.2.2 Influence of impact velocity

Similarly, the variation of erosion rate of unfilled and SiC filled composites with impact velocity is shown in Figure 3. Erosion trials are conducted at five different impact velocities.

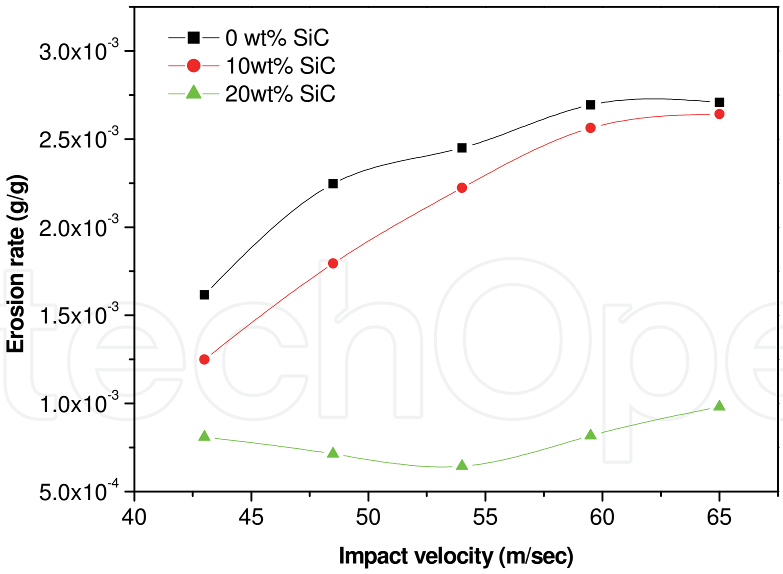

(Impingement angle: 60°, stand-off distance: 75mm and erodent size: 450μm)

Fig. 3. Influence of impact velocity on erosion rates of composites

It is seen, in the Figure 3 that for all the composite samples, the erosion rates gradually increases with the increase in impact velocity from 43m/sec to 65m/sec respectively. The increase in erosion rate with increase in impact velocity can be attributed to increased penetration of particles on impact as a result of dissipation of greater amount of particle thermal energy to the target surface. This leads to more surface damage, enhanced sub-critical crack growth etc. and consequently to the reduction in erosion resistance.

3.3 Taguchi analysis and response optimization

The analysis is made using the computational software MINITAB 15. Table 2 shows the experimental design using L_{27} orthogonal array. The overall mean for the S/N ratio of erosion rate is found to be 61.92db for erosion rate is mentioned in the response table.

Expt. No.	Impact Velocity (A)(m/s)	SiC content (B) (%)	Impingement angle (C) (Degree)	Stand-off Distance (D)(mm)	Erodent size (E) (µm)	Erosion rate (Er) (g/g)	S/N Ratio (db)
1	43	0	30	65	250	0.0003303	69.6224
2	43	0	60	75	350	0.0002466	72.1588
3	43	0	90	85	450	0.0001246	78.0908
4	43	10	30	75	350	0.0004458	67.0165
5	43	10	60	85	450	0.0002775	71.1347
6	43	10	90	65	250	0.0023721	52.4974
7	43	20	30	85	450	0.0006133	64.2461
8	43	20	60	65	250	0.0003333	69.5424
9	43	20	90	75	350	0.0006175	64.1873
10	54	0	30	75	450	0.0014625	56.6981
11	54	0	60	85	250	0.0028121	51.0194
12	54	0	90	65	350	0.0027000	51.3727
13	54	10	30	85	250	0.0000917	80.7558
14	54	10	60	65	350	0.0022625	52.9082
15	54	10	90	75	450	0.0027392	51.2476
16	54	20	30	65	350	0.0005450	65.2721
17	54	20	60	75	450	0.0001229	78.2078
18	54	20	90	85	250	0.0007804	62.1535
19	65	0	30	85	350	0.0024783	52.1171
20	65	0	60	65	450	0.0045143	46.9082
21	65	0	90	75	250	0.0031857	49.9359
22	65	10	30	65	450	0.0004354	67.2217
23	65	10	60	75	250	0.0009611	60.3442
24	65	10	90	85	350	0.0004091	67.7625
25	65	20	30	75	250	0.0002840	70.9336
26	65	20	60	85	350	0.0034362	49.2785
27	65	20	90	65	450	0.0035105	49.0927

Table 2. Experimental design using L_{27} orthogonal array

The Effect of control factors on erosion rate is shown in Figure 4. It is observed from response graph that the combination of factors settings are A_1, B_3, C_1, D_3 and E_1 have been found to be the optimum factor level for the erosion rate is concerned on the basis of smaller-the-better characteristics. The corresponding interaction graphs are plotted in the Figures 5a-c.

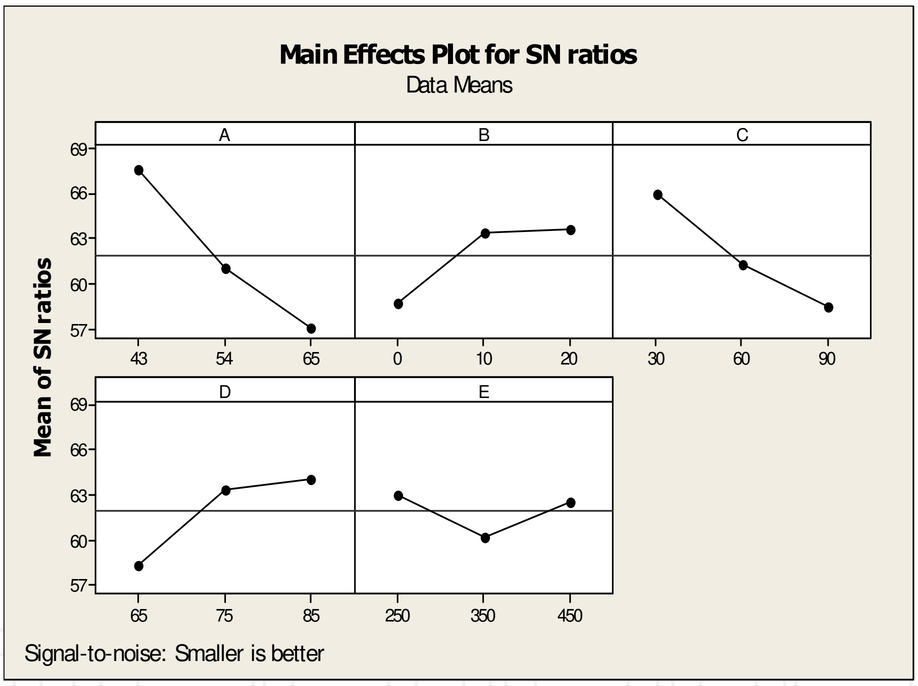

Fig. 4. Effect of control factors on erosion rate

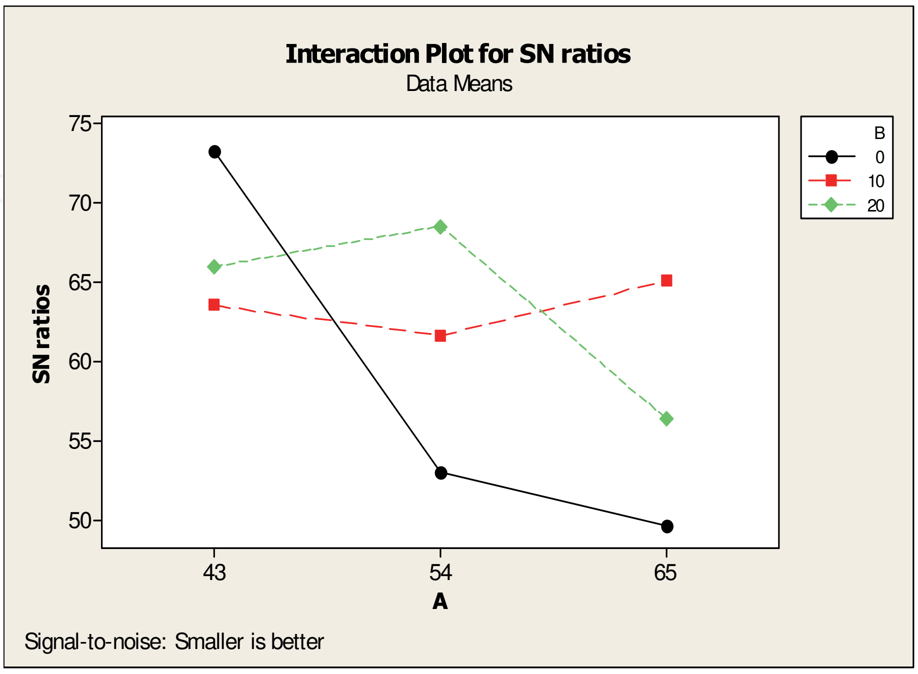

Fig. 5a. Interaction graph between factor A and factor B (A×B) for erosion rate

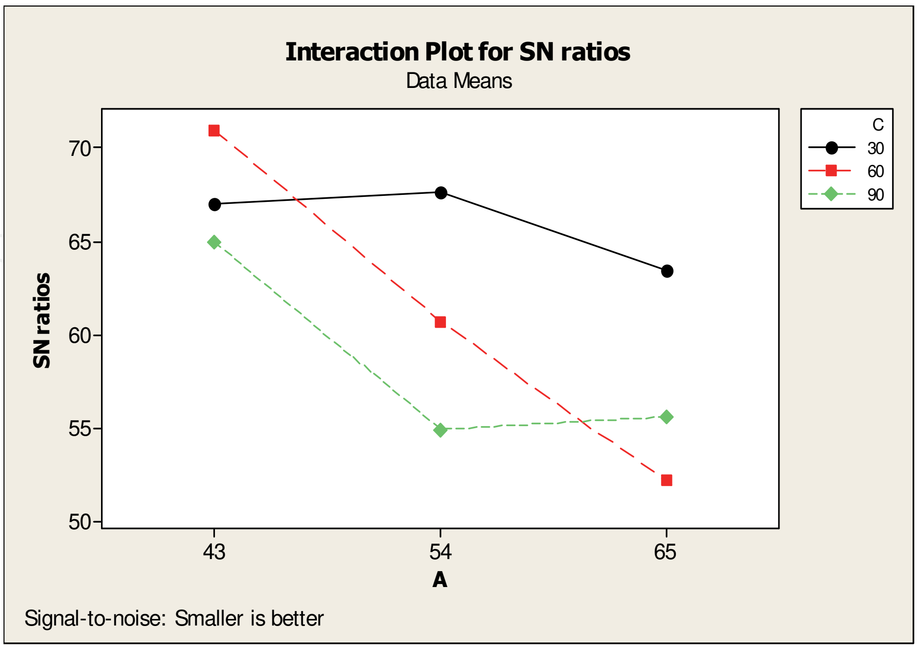

Fig. 5b. Interaction graph between factor A and factor C (A×C) for erosion rate

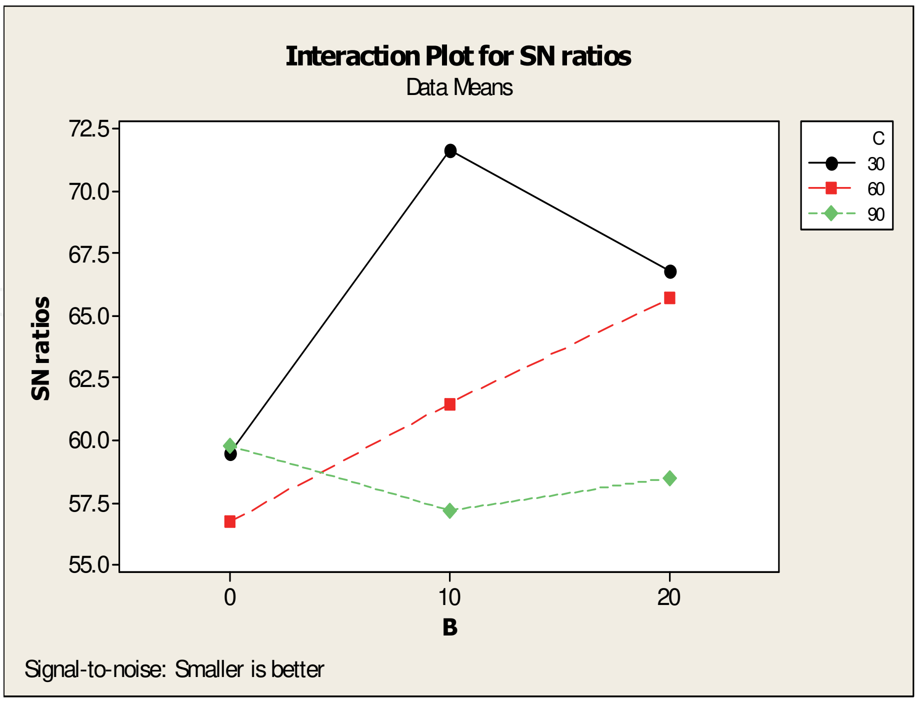

Fig. 5c. Interaction graph between factor B and factor C (B×C) for erosion rate

3.4 Surface morphology

The erosion wear mechanisms of SiC filled glass fiber reinforced polyester composites eroded surfaces are observed as per Taguchi experimental design by scanning electron microscopy (SEM). Figure 6a and 6b shows the SEM of eroded composite sample studied at lower impingement angle (see Table 2, Experiment 4). The random distribution of SiC fillers on the composite surface and removable of matrix material on the composite surface are clearly observed from the figures. Figure 6c shows the increase in erosion rate with higher impingement angle (90°) for 10wt% of SiC filled glass-polyester composites (see Table 2, Experiment 6). Figure 6d shows a hole formed after SiC particle was removed from the surface. The inside surface of the hole seemed very smooth and clear which indicated that SiC particles debonded from the matrix surface with the propagation of interfacial cracks due in part to the poor interfacial bond strength (see Table 2, Experiment 11). This is due to the increase in impact velocity from 43m/s to 54m/s and more energy to chip-off the target material.

Similarly Figure 6e and 6f show the fibers are protruded above the worn surface due to SiC particles are removed from the upper surface of the composites. However, there is a significant difference between Figures 6e and 6f due to the change in impingement angle and change in impact velocity. Thus, after the removal of the matrix material, there could be a layer of glass fiber and SiC particulates bonded on the matrix material. This indicated the favorable effect of good interfacial bond strength on the wear performance for the composites which helped prolong the lifetime of the SiC particulates to bear erosion and protect the matrix material before it was removed away. It has been reported by few of researchers that the impact on brittle materials at an oblique angle produced radial cracks at an angle to the surface and they can contribute to only matrix material loss (Scattergood et al., 1981; Lawn, 1993). Radial cracks can also contribute to material removal when they drive through a relatively thin wall. In such a case, the material loss will occur without the formation of a lateral crack. Due to the above wear mechanism the larger erodent produce

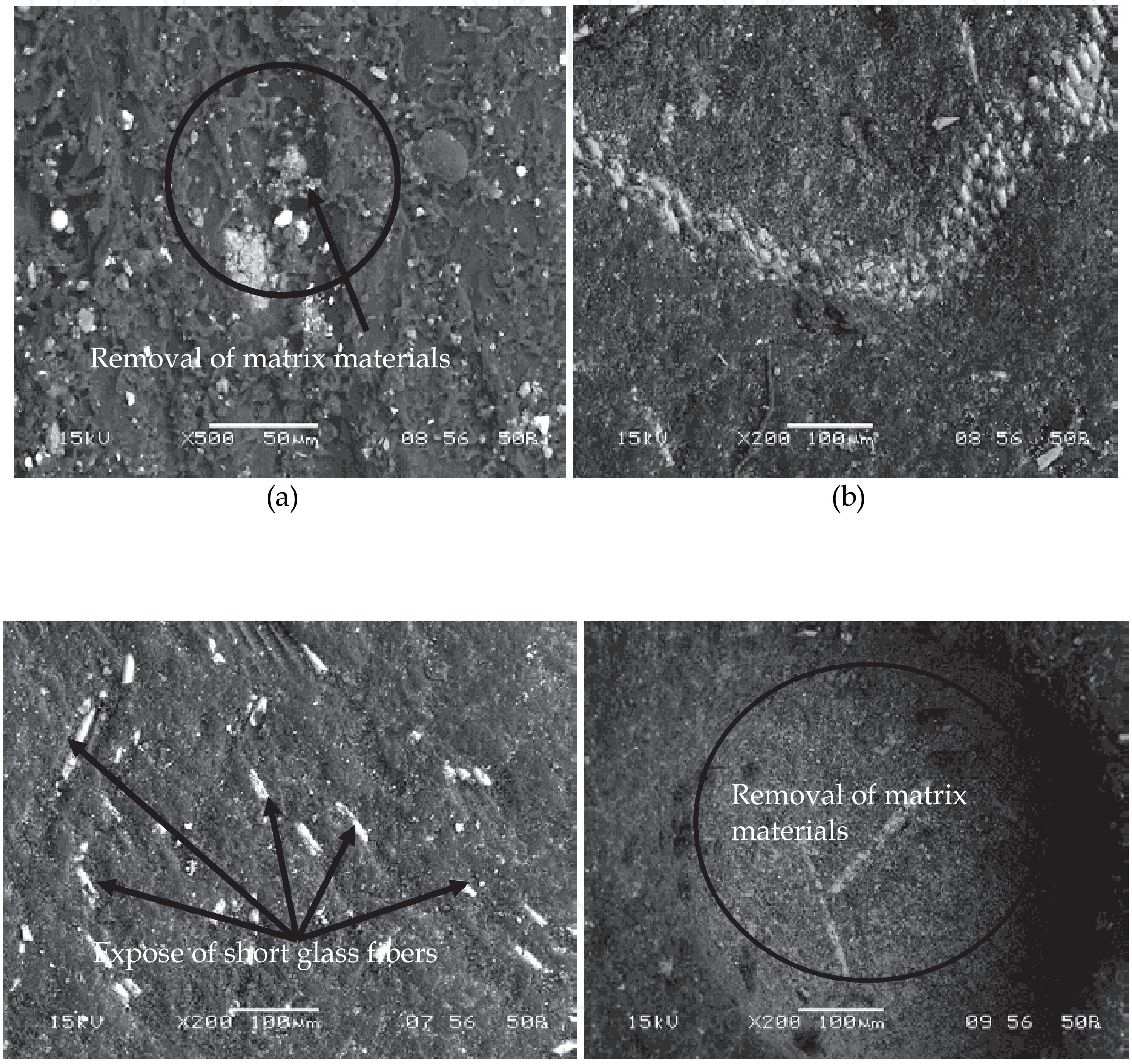
Removal of matrix materials
15kV X500 50μm 08 56 50R
15kV X200 100μm 08 56 50R
Expose of short glass fibers
15kV X200 100μm 07 56 50R
Removal of matrix materials
15kV X200 100μm 09 56 50R

(a) (b)

(c) (d)

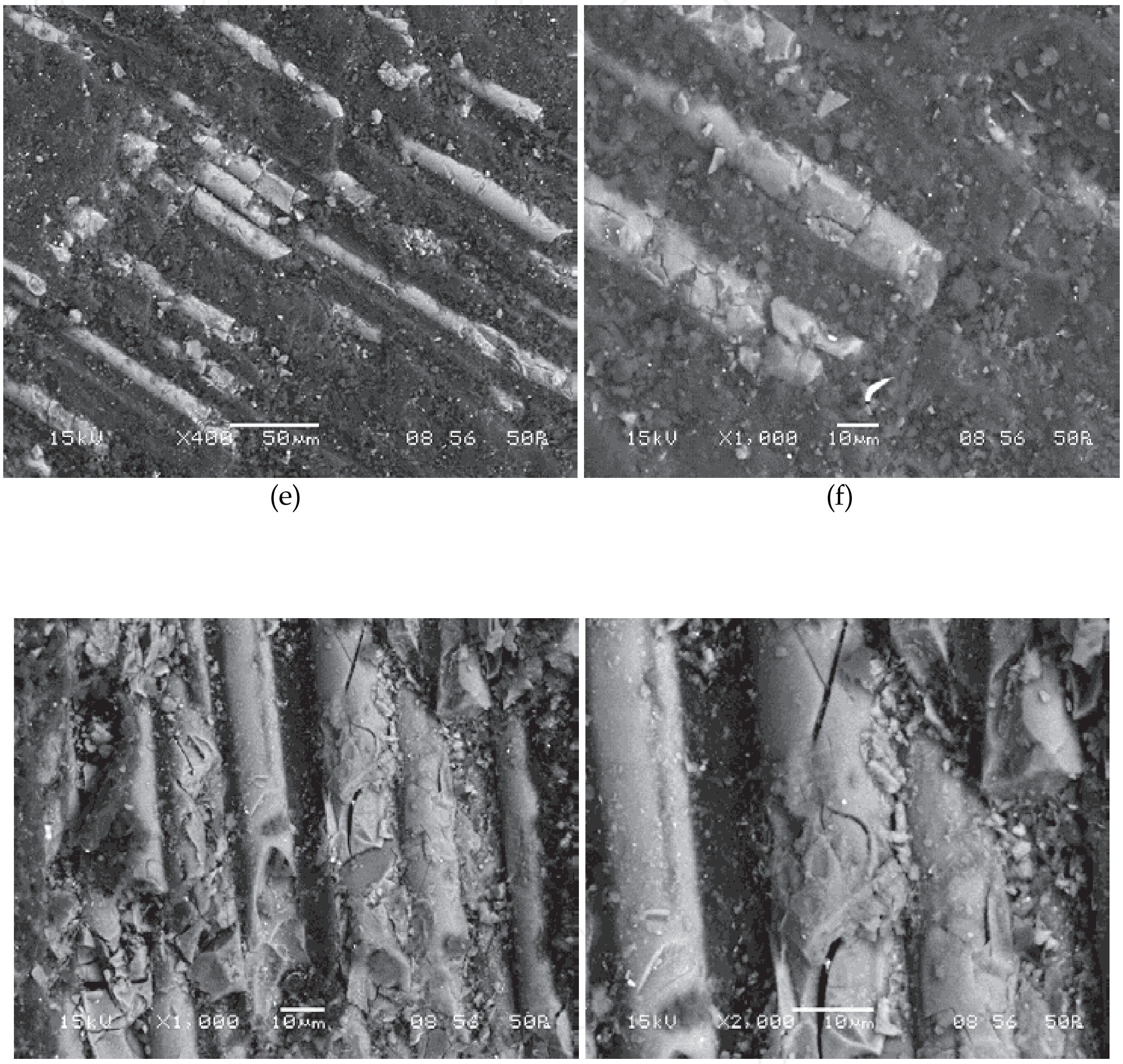

(e) (f)

(g) (h)

Fig. 6. SEM micrographs of the eroded glass fiber-polyester composites filled with SiC

deeper radial cracks on the eroded surfaces. The tendency for material loss to occur from radial cracking should increase with increase in erodent size (Lee et al., 2005; Milman et al., 1999). However, with the increasing content of the SiC particles in the composites from 10wt% to 20wt%, the wear rate of the composites increased gradually, reached a maximum and then declined gradually. With the further increase in impact velocity from 54m/sec to 65m/sec for 20wt% SiC filled short glass fiber reinforced polyester composites the material removal on the surface is more but the erosion resistance become more as compared with other particulate filled glass-polyester composites as shown in Figure 6g and 6h (see Table 2, Experiment 25). In the present study, the matrix material is removed from the composite surface due to continuous impact of erodent particles with sharp angles and high impact velocity, but the reinforcing glass fibers and SiC particulates are removed slowly then the matrix material. This may be due to the inclusions of high hardness of SiC particles.

3.5 ANOVA and the effects of factors

The results of the experimental trials were investigated using the ANOVA statistical analysis method. Table 3 shows the results of the ANOVA with the erosion rate (E_r) for SiC filled short glass fiber reinforced polyester composites. The objective of ANOVA is to analyze the influence of impact velocity (A), SiC content (B), impingement angle (C), stand-off distance (D) and erodent size (E) on the total variance of the results. This analysis was undertaken for a level of significance of 5% that is for a level of confidence of 95%.

From Table 3, it is concluded that impact velocity (p = 0.191), impingement angle (p = 0.365), stand-off distance (p = 0.470) and SiC content (p = 0.539) have great influence on the erosion rate. The interactions of impact velocity and SiC content (p = 0.283) has most significant effect on erosion rate but the factor erodent size (p = 0.828), interaction between SiC content and impingement angle (p = 0.717) and impact velocity and impingement angle (p = 0.684) have less significant contribution on erosion rate.

Source	DF	Seq SS	Adj SS	Adj MS	F	P
A	2	510.00	510.00	255.00	2.58	0.191
B	2	143.49	143.49	71.75	0.73	0.539
C	2	258.94	258.94	129.47	1.31	0.365
D	2	181.24	181.24	90.62	0.92	0.470
E	2	39.22	39.22	19.61	0.20	0.828
A×B	4	733.23	733.23	183.31	1.85	0.283
B×C	4	213.85	213.85	53.46	0.54	0.717
A×C	4	237.42	237.42	59.35	0.60	0.684
Error	4	395.79	395.79	98.95		
Total	26	2713.18				

Table 3. ANOVA table for erosion rate

3.6 Confirmation experiment

To determine the optimal conditions and to compare the result with the predicted performance, it is necessary to perform a confirmation experiment. If the generated design fails to meet the predicted requirement, the process must be reiterated using a new system unit and finally the required criteria are satisfied. The confirmation experiment is performed by conducting a new series of test condition in combination of the significant factors and their respective interaction levels on erosion rate as reported in Table 3. The final step is to predict and verify the improvement of the erosion resistance. The predictive value $\bar{\eta}_1$ using the optimal levels of the input parameters can be calculated as:

$$\bar{\eta}_1 = \bar{T} + (\bar{A}_2 - \bar{T}) + (\bar{B}_2 - \bar{T}) + [(\bar{A}_2\bar{B}_2 - \bar{T}) - (\bar{A}_2 - \bar{T}) - (\bar{B}_2 - \bar{T})] + (\bar{C}_3 - \bar{T}) + (\bar{D}_2 - \bar{T}) + (\bar{E}_3 - \bar{T}) \tag{3}$$

$\bar{\eta}_1$: Predicted average
$\bar{T}$: Overall experimental average
$\bar{A}_2, \bar{B}_2, \bar{C}_3, \bar{D}_2$ and $\bar{E}_3$ Mean response for factors and interactions at designated levels.
By combining like terms, the equation reduces to

$$\bar{\eta}_1 = \bar{A}_2\bar{B}_2 + \bar{C}_3 + \bar{D}_2 + \bar{E}_3 - 3\bar{T} \tag{4}$$

After solving the above predictive equation the erosion rate is found to be $\bar{\eta}_1 = 57.61\,\text{dB}$ and the experimental result is 56.33 dB. The resulting model seems to be capable of predicting wear rate to a reasonable level of accuracy. An error of 2.22% for the S/N ratio of wear rate is observed. This validates the development of the mathematical model for predicting the measures of performance based on knowledge of the input parameters.

4. Conclusions

1. The present work successfully fabricated SiC filled short glass fiber reinforced polyester composites by simple hand-lay-up techniques and also showed that it was feasible to add SiC particles to the glass-polyester resin composites to improve their erosion resistance.
2. The particle filled composites show good tribological properties as compared with the unfilled glass fiber reinforced polyester composites. The erosion rate for 20wt% SiC filled composites shows superior erosion resistance as compared with the rest of the filled and unfilled composites.
3. The variation of erosion rate with impingement angles, the material loss is dictated mainly more at 60° impingement angles for unfilled composites and for filled composites the maximum erosion resistance show around 45° impingement angle both in experimental and finite element simulated results.
4. On comparision with the experimental results, the FE model (ANSYS/AUTO-DYN) is much closer to the experimental results. The major advantages of simulated results are during experimental study it is very difficult to analysis the flow direction and particularly at low impingement angle most of the erodent particles are sliding on the target composite materials instead of reback of erodent particles from the composite surface. However, finite element simulated model can be easily implemented to measure the residual stress and the depth of penetration which is difficult to determine by experimental method.

5. In eroded samples observed in SEM shows mostly two types of wear mechanisms i.e. micro-cutting and micro-ploughing actions. As far as SiC filled glass polyester composite is concerned the matrix material is removed at faster rate from the composite surface due to continuous impact of erodent particles with sharp angles and high impact velocity, but the reinforcing glass fibers and SiC particulates are removed slowly then the matrix material. This may be due to the inclusions of high hardness of SiC particles.

5. Acknowledgement

The authors are grateful to the financial supports of the research project Ref. No. SR/FTP/ETA-49/08 by Department of Science and Technology, India.

6. References

Bahadur, S. & Tabor, D. (1985). Role of fillers in friction and wear behaviour of HDPE In: *Polymer wear and its control*, Volume 287-268 (L.H. Lee (ed.) ACM symposium series, Washington DC.

Bahadur, S.; Fu, Q.; & Gong, D. (1994). The effect of reinforcement and the synergism between CuS and carbon fiber on the wear of nylon, *Wear*, Vol. 178, pp. 123-130.

Briscoe, B. J.; Pogosion, A. K.; & Tabor, D. (1974). The friction and wear of high Density polyethylene; the action of lead oxide and copper oxide fillers, *Wear*, Vol.27, pp. 19-34.

Budinski, K.G. (1997). Resistance of particle abrasion to selected plastics, *Wear*, Vol. 203–204, pp. 303–309.

Chand, N.; Naik, A.M.; & Neog i , S. (2000). Three-body abrasive s wear of short glass fiber polyester composite, *Wear*, Vol. 242, pp.38–46.

ElTobgy, M. S.; Ng, E. & Elbestawi, M. A. (2005). Finite Element Modeling of Erosive Wear, *International Journal of Machine Tools and Manufacture*, Vol. 45, pp. 1337-1346.

Hutchings, I. M. (1992). Ductile brittle transitions and wear maps for the erosion and abrasion of brittle materials, *Journal of Physics D: Applied Physics*, Vol. 25, pp. A212-A221.

Kishore.; Sampathkumaran, P.; Seetharamu, S.; Vynatheya, S.; Murali, A.; Kumar, R. K. (2000). SEM observations of the effect of velocity and load on the slide wear characteristics glass-fabric-epoxy composites with different fillers, *Wear*, Vol. 237, pp. 20-27.

Lawn, B. (1993). *Fracture in Brittle Solids*, 2nd ed., Cambridge University Press, Cam-bridge, UK.

Lee, S. H.; Lee, Y. I.; Kim, Y.W.; Xie, R. J.; Mitomo, M. & Zhan, G. D. (2005). Mechanical Properties of Hot-Forged Silicon Carbide Ceramics, *Scripta Materialia*, Vol. 52, pp. 153-156.

Milman, Y.V.; Chugunova, S. I.; Goncharova, I. V.; Chudoba, T.; Lojkowski, W. & Gooch, W. (1999). Temperature Dependence of Hardness in Silicon-Carbide Ceramics with Different Porosity, *International Journal of Refractory Metals and Hard Materials*, Vol. 17, No. 5, pp. 361-368.

Nordsletten, L.; Hogasen, A.; Konttinen, Y.; Santavirta, S.; Aspenberg, P.; Aasen, A. (1996). Human monocytes stimulation by particles of hydroxyapatite, silicon carbide, and diamond: in vitro studies of new prosthesis coatings. *Biomaterials*, Vol. 17, pp.1521–1527.

Patnaik, A.; Biswas, S.; Kaundal, R.; Satapathy, A. (2011). Damage Assessment of Short Glass Fiber Reinforced Polyester Composites: A comparative Study, *Composites*, In Tech open access publisher, ISBN 978-953-307-1100-7.

Peace, G. S. (1993). *Taguchi methods: A hand-on approach*. Reading, MA: Addison-Wesley.

Phadke, M. S. (1989). *Quality engineering using robust design*. Englewood Cliffs, NJ: Prentice-Hall.

Routbort, J. L.; Gulden, M. E. & Marshall, E. (1981). Particle Size Distribution Effects on the Solid Particle Erosion of Brittle Materials, *Wear*, Vol. 71, pp. 363-373.

Ruff, A.W.; Ives, L.K. (1975). Measurement of solid particle velocity in erosive wear, *Wear*, Vol. 35, pp. 195–199.

Scattergood, R. O.; Routbort, J. L. & Turner, A. P. L. (1981). Velocity and Size Dependence of the Erosion Rates in Silicon, *Wear*, Vol. 67, pp. 227-232.

Strzepa, P.; Zamirowski, E. J.; Kupperman, J. B.; Goretta, K. C. & Routbort, J. L. (1993). Indentation, Erosion and Strength Degradation of Silicon-Alloyed Pyrolytic Carbon, *Journal of Materials Science*, Vol. 28, pp. 5917–5921.

Tanaka, K., (1986). Effect of various fillers on the friction and wear of PTFE-based composites, In: *Friction and Wear of Polymer composites,* Vol. 205, pp. 137-174, (Friedrich K editor), Elsevier, Amsterdam.

Tripathy, B. S.; Furey, M.J.; (1993). Tribological behaviour of unidirectional graphite-epoxy and carbon-PEEK composites. *Wear*, Vol. 162–164, pp. 385–391.

Tsuda, K.; Kubouchi, M.; Sakai, T.; Saputra, A. H. & Mitomo, N. (2006). General Method for Predicting the Sand Erosion Rate of GFRP, *Wear*, Vol. 260, pp. 1045-1052.

Wang, J.; Gu, M.; Songhao, Ge. S. (2003). The role of the influence of MoS2 on the tribological properties of carbon fiber reinforced Nylon 1010 composites, *Wear,* Vol. 255, pp. 774-779.

Woytowitz, P. J. & Richman, R. H. (1999). Modeling of Damage from Multiple Impacts by Spherical Particles, *Wear*, Vol. 233-235, pp. 120-133.

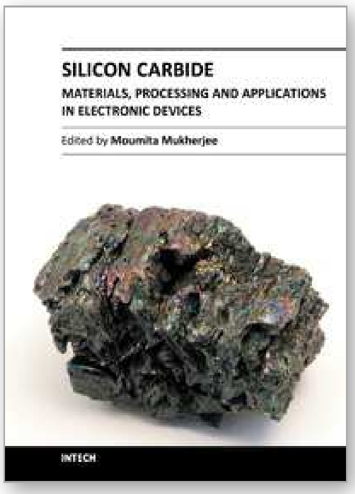

SILICON CARBIDE
MATERIALS, PROCESSING AND APPLICATIONS IN ELECTRONIC DEVICES
Edited by Moumita Mukherjee
INTECH

Silicon Carbide - Materials, Processing and Applications in Electronic Devices
Edited by Dr. Moumita Mukherjee

ISBN 978-953-307-968-4
Hard cover, 546 pages
Publisher InTech

Published in print edition October, 2011

Silicon Carbide (SiC) and its polytypes, used primarily for grinding and high temperature ceramics, have been a part of human civilization for a long time. The inherent ability of SiC devices to operate with higher efficiency and lower environmental footprint than silicon-based devices at high temperatures and under high voltages pushes SiC on the verge of becoming the material of choice for high power electronics and optoelectronics. What is more important, SiC is emerging to become a template for graphene fabrication, and a material for the next generation of sub-32nm semiconductor devices. It is thus increasingly clear that SiC electronic systems will dominate the new energy and transport technologies of the 21st century. In 21 chapters of the book, special emphasis has been placed on the â€œmaterialsâ€ aspects and developments thereof. To that end, about 70% of the book addresses the theory, crystal growth, defects, surface and interface properties, characterization, and processing issues pertaining to SiC. The remaining 30% of the book covers the electronic device aspects of this material. Overall, this book will be valuable as a reference for SiC researchers for a few years to come. This book prestigiously covers our current understanding of SiC as a semiconductor material in electronics. The primary target for the book includes students, researchers, material and chemical engineers, semiconductor manufacturers and professionals who are interested in silicon carbide and its continuing progression.

Sandhyarani Biswas, Amar Patnaik and Pradeep Kumar (2011). Silicon Carbide Filled Polymer Composite for Erosive Environment Application: A Comparative Analysis of Experimental and FE Simulation Results, Silicon Carbide - Materials, Processing and Applications in Electronic Devices, Dr. Moumita Mukherjee (Ed.), ISBN: 978-953-307-968-4, InTech, Available from: http://www.intechopen.com/books/silicon-carbide-materials-processing-and-applications-in-electronic-devices/silicon-carbide-filled-polymer-composite-for-erosive-environment-application-a-comparative-analysis-

INTECH
open science | open minds

InTech Europe
University Campus STeP Ri
Slavka Krautzeka 83/A
51000 Rijeka, Croatia

InTech China
Unit 405, Office Block, Hotel Equatorial Shanghai
No.65, Yan An Road (West), Shanghai, 200040, China
中国上海市延安西路65号上海国际贵都大饭店办公楼405单元

www.intechopen.com

Phone: +385 (51) 770 447
Fax: +385 (51) 686 166
www.intechopen.com

Phone: +86-21-62489820
Fax: +86-21-62489821